



# The role of the N-terminal amphipathic helix in bacterial YidC: Insights from functional studies, the crystal structure and molecular dynamics simulations

Karol J. Nass<sup>a,1</sup>, Ioana M. Ilie<sup>b,\*</sup>, Manfred J. Saller<sup>c,2</sup>, Arnold J.M. Driessen<sup>c</sup>, Amedeo Caflisch<sup>b</sup>, Richard A. Kammerer<sup>d</sup>, Xiaodan Li<sup>d,\*</sup>

<sup>a</sup> Photon Science Division, Paul Scherrer Institute, Forschungstrasse 111, 5232 Villigen PSI, Switzerland

<sup>b</sup> Department of Biochemistry, University of Zurich, Winterthurerstrasse 190, CH-8057 Zurich, Switzerland

<sup>c</sup> Department of Molecular Microbiology, Groningen Biomolecular Sciences and Biotechnology Institute, Nijenborgh 7, 9727 AG Groningen, The Netherlands

<sup>d</sup> Laboratory of Biomolecular Research, Division of Biology and Chemistry, Paul Scherrer Institute, Forschungstrasse 111, 5232 Villigen PSI, Switzerland

## ARTICLE INFO

### Keywords:

YidC insertase and chaperone  
Interaction of YidC and Sec translocon  
Recognition helix  
X-ray crystallography  
Molecular dynamics (MD) simulations

## ABSTRACT

The evolutionary conserved YidC is a unique dual-function membrane protein that adopts insertase and chaperone conformations. The N-terminal helix of *Escherichia coli* YidC functions as an uncleaved signal sequence and is important for membrane insertion and interaction with the Sec translocon. Here, we report the first crystal structure of *Thermotoga maritima* YidC (TmYidC) including the N-terminal amphipathic helix (N-AH) (PDB ID: 6Y86). Molecular dynamics simulations show that N-AH lies on the periplasmic side of the membrane bilayer forming an angle of about 15° with the membrane surface. Our functional studies suggest a role of N-AH for the species-specific interaction with the Sec translocon. The reconstitution data and the superimposition of TmYidC with known YidC structures suggest an active insertase conformation for YidC. Molecular dynamics (MD) simulations of TmYidC provide evidence that N-AH acts as a membrane recognition helix for the YidC insertase and highlight the flexibility of the C1 region underlining its ability to switch between insertase and chaperone conformations. A structure-based model is proposed to rationalize how YidC performs the insertase and chaperone functions by re-positioning of N-AH and the other structural elements.

## 1. Introduction

YidC belongs to the YidC/Alb3/Oxa1 membrane protein family which is evolutionary conserved from archaea to man [1]. The proteins of this family play an important role in the insertion and folding of membrane proteins in the bacterial, thylakoidal, mitochondrial inner membranes and the eukaryotic endoplasmic reticulum [2–4]. Two conserved structural elements have been identified in all YidC proteins. First, the hydrophilic groove within the transmembrane domain (TMD), consisting of the transmembrane helices TM2 to TM6, which represents the catalytic center of the protein. Second, the C1 region connecting TM2 and TM3, which consists of two helices (CH1 and CH2) connected by a short loop forming a hairpin-like structure (Fig. 1). Though sharing rather low sequence similarity, the hydrophilic groove and its ability to

form lipid-mediated homo- or hetero-oligomers to promote the efficient protein translocation [2,4] are conserved among the family members. The most studied protein from this family is YidC from *Escherichia coli* (EcYidC). Depletion of the YidC protein results in cell death due to the defective assembly of energy-transducing membrane complexes [5], this makes the YidC protein an attractive antibiotic target.

The YidC chaperone is an integral part of the holo translocon (HTL), which folds and assembles multipass transmembrane proteins, as shown in the low-resolution cryo-EM structure of the SecYEG-SecDFYajC-YidC complex [6–8]. The YidC chaperone facilitates the removal of non-mature membrane protein substrates from the lateral gate of the SecY protein, releasing the substrates into the lipid bilayer [9,10]. HTLs likely exist in a dynamic manner within the lipid bilayer for accommodating the diverse substrates and improving insertion efficiency [11,12].

\* Corresponding authors.

E-mail addresses: [i.m.ilie@uva.nl](mailto:i.m.ilie@uva.nl) (I.M. Ilie), [xiao.li@psi.ch](mailto:xiao.li@psi.ch) (X. Li).

<sup>1</sup> Contributed equally.

<sup>2</sup> Current affiliation: Lava Therapeutics NV, Yalelaan 60, 3584CM Utrecht, The Netherlands.

The hydrophilic groove is open towards the lipid bilayer and the cytoplasm but closed on the periplasmic side [13,14]. High B-factor values have been reported for the C1 region, indicating that this region fluctuates greatly near cytoplasmic bilayer surface, as also confirmed by the MD simulations [13]. The C1 region flexibility is required for the YidC insertase activity [15] and for YidC interactions with SecYEG [16]. Notably, the YidC protein from Gram-negative bacteria contains an additional N-terminal helix (TM1) [17] and a  $\beta$ -sandwich domain (P1) between TM1 and TM2. Replacement of the N-terminal helix by the cleavable signal peptide doesn't affect the function of YidC suggesting that the helix acts as an uncleaved signal sequence [17]. Deletion of the N-terminal helix compromises the insertion function of the YidC insertase, suggesting a recognition helix function for this helix [18]. Furthermore, *in vitro* site-directed and para-formaldehyde cross-linking experiments identified the N-terminal helix of the EcYidC as a major contact site with the Sec translocon and the C1 region as an additional contact site for the Sec translocon [10]. The low-resolution cryo-EM structure of the *E. coli* SecYEG-SecDFYajC-YidC HTL indicates that the N-terminal helix intercalates at the lateral gate of the empty SecY and aligns the YidC hydrophilic groove to the lateral gate of SecY, yet this helix is not visible in this structure [8]. Consequently, the hydrophilic groove of YidC and the lateral gate of SecY constitute a fusion protein-conducting channel with unique properties [10,19]. The fusion protein-conducting channel has a smaller pore size with less hydrophobicity and higher anion selectivity in comparison to the SecY channel alone. Furthermore, the fusion protein-conducting channel lowers the energy barrier for substrate releasing to the lipid bilayer [8,20–24].

Here, we address the structural and functional roles of the N-terminal amphipathic helix (N-AH) of *Thermotoga maritima* YidC. We present a TmYidC crystal structure in which the N-terminal helix is visible for the first time (PDB ID: 6Y86). The helix is tilted on the membrane surface and is amphipathic with polar residues segregated on one side and hydrophobic residues facing the membrane. Functional studies with chimeric proteins of EcYidC and TmYidC provide evidence that N-AH is important for the species-specific interaction with SecY. Molecular dynamics simulations reveal that the angle between the axis of N-AH and the membrane surface is about 15° and that its N-terminus is embedded in the membrane acting as a recognition helix. The superimposition of TmYidC with the known YidC structures yields a root mean square deviation of 3.3 Å from the active structure of the gram-positive *Bacillus*

*halodurans* YidC insertase (BhYidC), suggesting an active TmYidC insertase conformation, consistent with our reconstitution data. Our combined experimental and computational study shows that N-AH, the EH1 helix and the C1 region of YidC protein can adopt different conformations for insertion and interaction with the Sec translocon. We propose a structure-based model characterizing the insertase and chaperone conformations of YidC protein.

## 2. Results

### 2.1. Functional analysis of N-AH from *Thermotoga maritima* YidC

Based on crosslinking data, we propose that N-AH of YidC needs to interact with SecY to allow YidC to perform its function as a chaperone, thereby suggesting a species-specific functional role of N-AH. To test this hypothesis, EcYidC, TmYidC and a TmYidC chimera containing the N-terminal helix of EcYidC (YidC61) (Fig. 2a) were expressed in *E. coli* FTL10 (see Supplementary information Table S1). In this strain, the *yidC* gene is under the control of the *araBAD* promoter. Since EcYidC is essential for cell viability, the growth of *E. coli* FTL10 is dependent on the presence of arabinose in the medium [25]. For the complementation assays, plasmids pTrcTmaHis and pTrc61-t396His (see Supplementary information Table S2) were introduced into the FTL10 strain and cells were grown with glucose instead. In YidC61, the N-terminal 47 amino acids including N-AH of TmYidC was replaced with the N-terminal 61 residues of EcYidC. The topology of these proteins is shown in Fig. 2a. In addition, the EcYidC (pTrcyidC) and the empty vector (pTrc99A) were used as positive and negative controls, respectively (see Supplementary information Table S2). Transformed cells were tested for growth in liquid Luria-Bertani (LB) medium. As expected, all cells were viable in the LB medium supplemented with arabinose (Fig. 2b, upper panel). However, under conditions, which repress the expression of chromosomal *yidC* (glucose, IPTG), EcYidC (positive control) and YidC61 complemented the *E. coli* FTL10 growth defect (Fig. 2b, lower panel). Cells transformed with the empty vector and TmYidC showed poor growth under these conditions. One of the possible reasons for the lack of YidC complementation by TmYidC is that N-AH of TmYidC is not able to interact with *E. coli* SecY (EcSecY) to form a HTL, which can insert and fold the substrates more efficiently and is required for growth. Western blot experiments using purified EcSecY, EcYidC and TmYidC confirm the

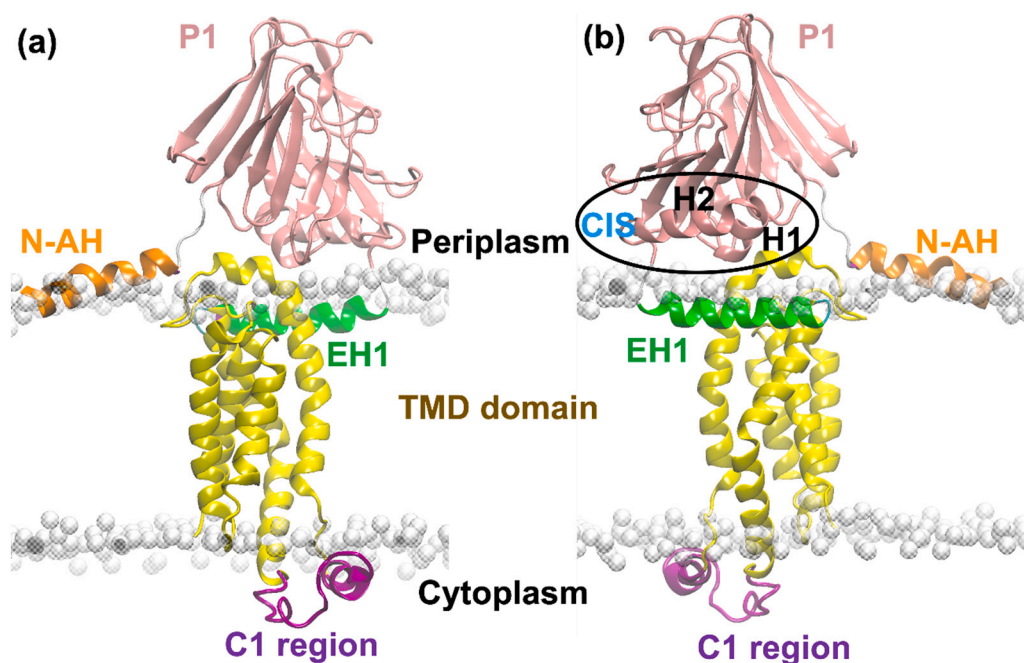


**Fig. 1.** Overall structure of the TmYidC. (a) Front view of TmYidC. (b) Back view of TmYidC (PDB ID: 6Y86). N-AH: orange (residues 1–19), P1: pink (23–225), EH1: green (226–244), TM region: yellow (TM2 (248–280), TM3–TM6 (317–424)) and C1 region: magenta (282–308). A highly conserved interface structure (CIS) formed by packing C-terminal helix1 (H1) and helix2 (H2) against the  $\beta$ -supersandwich via hydrophobic interactions in P1 domain is shown in a black ellipse. The phosphorus atoms in the membrane are shown as white spheres. (For interpretation of the references to color in this figure legend, the reader is referred to the web version of this article.)

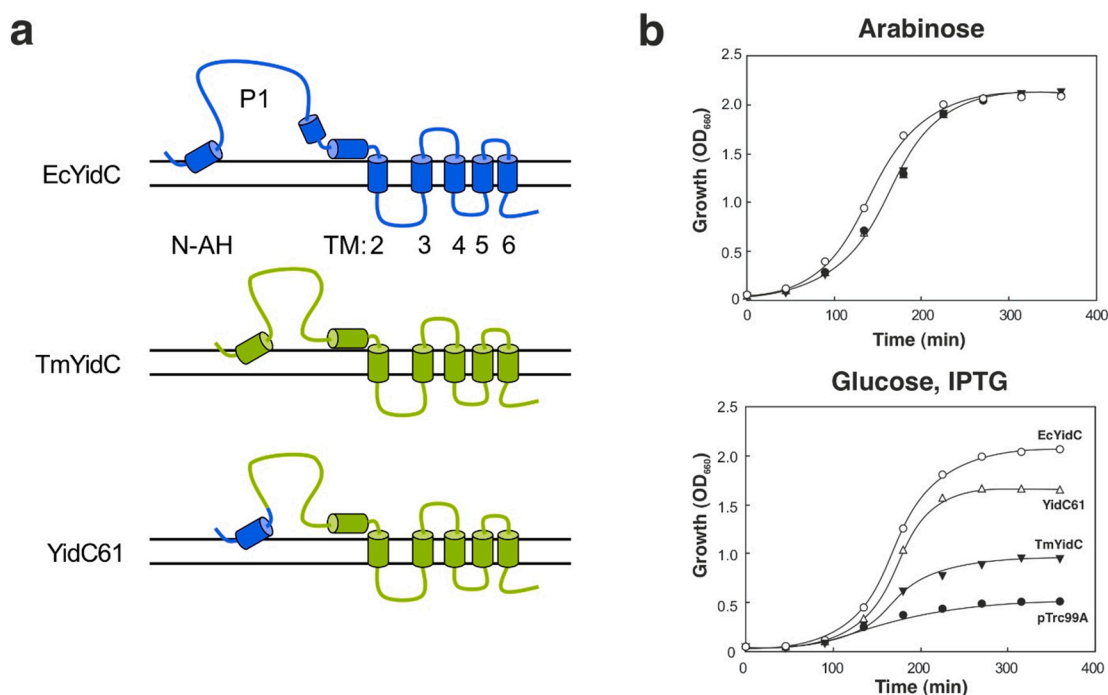


**Fig. 2.** Complementation of the growth defect of an *E. coli* YidC depletion strain by chimeric *E. coli* and *T. maritima* YidC proteins. (a) Topology models of the EcYidC (blue) and the TmYidC (green) proteins. The  $\alpha$ -helical regions (TM) and hydrophilic helices H1 and H2) are represented by cylinders, solid lines indicate soluble terminal and loop regions. YidC61 is a chimeric protein consisting of the N-AH from EcYidC (N-terminal, blue) and TmYidC (C-terminal, green). (b) The *E. coli* FTL10 cells were grown in a medium supplemented with either 0.5% (wt/vol) arabinose (top panel) or glucose and 50  $\mu$ M IPTG (bottom panel). Cells containing the empty plasmid pTrc99A (filled circles) or plasmids for the expression of EcYidC (open circles), YidC61 (open triangles) and TmYidC (filled triangles) were grown under induction and repression conditions. (For interpretation of the references to color in this figure legend, the reader is referred to the web version of this article.)

existence of a weak and transient interaction between EcSecY and endogenous EcYidC, but not when TmYidC is overexpressed (see Supplementary information Fig. S1). TmYidC can be expressed and purified from *E. coli* membrane demonstrating that its inability to complement growth cannot be explained by a lack of protein expression or a failure in membrane targeting. These data underscore the importance of N-AH for YidC activity and might reflect a species-specific function, for the interaction with SecY [10]. An alignment of different YidC proteins shows that N-AH of all gram-negative bacteria YidC share some similarities, yet the isoelectric point and the net charge of N-AH of EcYidC and TmYidC are different, i.e., 4.3 with one negatively charged residue and 8.5 with one positively charged residue, respectively (see Supplementary information Fig. S2).

## 2.2. The crystal structure of TmYidC and molecular dynamics simulations suggest that N-AH is a membrane recognition helix for the YidC insertase

We crystallized TmYidC using the vapor diffusion method in presence of the detergent dodecyl maltoside (DDM) and solved the structure by molecular replacement using the crystal structure of the P1 domain of TmYidC as search model (unpublished). The final model was refined to a resolution of 3.4 Å (Table 1). The asymmetric unit contains one TmYidC molecule. This data is consistent with size exclusion chromatography experiments showing TmYidC existing as a monomer in solution containing DDM (see Supplementary information Fig. S3). Structure analysis of TmYidC was carried out using published YidC structures [13,14,26–29].

The electron density of TmYidC has good resolution for residues 1–425 including the N-terminal amphipathic helix (residues 1–19). Residues 426–445 are not visible in the structure, indicating the flexibility of the C-terminus in the absence of the ribosome. Front and back view of the TmYidC structure are shown in Fig. 1a and b, respectively. The overall structure of TmYidC is well defined with all structural

**Table 1**  
Data collection and refinement statistics.

Data collection <sup>a</sup>	
Space group	P4 <sub>1</sub> 2 <sub>1</sub> 2
Cell dimensions	
<i>a</i> , <i>b</i> , <i>c</i> (Å)	122.6, 122.6, 97.1
$\alpha$ , $\beta$ , $\gamma$ (°)	90, 90, 90
Wavelength (Å)	1.0
Resolution (Å)	48.55–3.4
No. reflections	10,680
Completeness (%)	100 (100)
Redundancy	30.1 (24.7)
Mean I/ $\sigma$ I	13.7 (1.0)
R <sub>meas</sub> (%)	26.8 (495)
CC <sub>1/2</sub> (%)	99.8 (37.9)
Refinement	
Resolution range (Å)	20.0–3.4
No. reflections	10,052
R <sub>work</sub> /R <sub>free</sub>	26.2/30.1
No. atoms	
Protein	3487
Ligand/ion	0
Water	0
B-factors (Å <sup>2</sup> )	
Protein	154
R.m.s. deviations	
Bond lengths (Å)	0.004
Bond angles (°)	0.79
Ramachandran plot	
Favored (%)	87.5
Allowed (%)	22.5
Outliers (%)	0.0

<sup>a</sup> The numbers in parentheses are for the highest resolution shell.

elements visible (PDB ID: 6Y86). N-AH lays on the periplasmic

membrane face, forming a roughly 15-degree angle with the membrane and is located on the opposite side of the entrance to the hydrophilic groove. To further investigate the orientation of N-AH we performed molecular dynamics simulations starting from the crystal structure of TmYidC, which was first embedded in a POPE: POPG (3:1 ratio) bilayer to mimic the membrane environment of the YidC insertase. Ten independent simulations were carried out for a total sampling of 4  $\mu$ s. The results reveal that the tilt angle of N-AH with respect to the membrane surface (Fig. 3a) fluctuates in the  $[-10, +30]$  degrees interval (Fig. 3b) with an average of  $13^\circ$  and a standard deviation of  $\pm 8^\circ$ . The small standard error of the mean ( $\pm 3.4^\circ$ , evaluated as the standard deviation of the ten average values along the individual runs) suggests that the sampling has reached convergence. The secondary structure analysis shows that the N-AH preserves its  $\alpha$ -helical structure throughout the simulations except for the C-terminal residues Leu18-Phe19, which sample mainly coil- and bend-like conformations (Fig. 3c). The conformational changes (from insertase to chaperone) in N-AH extend beyond the timescale accessible by MD simulations.

In the crystal structure, the N-terminal amphipathic helix is tilted on the membrane surface and makes crystal contacts with two symmetry related molecules in the crystal packing. In this conformation, N-AH could fulfill its role as a recognition helix for localizing the YidC protein into the lipid bilayer, which is in agreement with deletion experiments [18] and the complementation experiment shown above. The molecular dynamics simulations of TmYidC in the lipid bilayer demonstrate that the N-terminus of N-AH is embedded in the membrane (Fig. 3d), thereby reinforcing the recognition helix role of N-AH.

### 2.3. The P1 domain and the EH1 helix of YidC can switch between insertase and chaperone conformations

The P1 domain of YidC forms a compact and rigid structure consisting

mainly of a  $\beta$ -sandwich, which accounts for more than half of the total amino acids of the protein [30], and is involved in the interaction with SecF [31]. The P1 domain of EcYidC is oriented towards the periplasmic membrane through its conserved C-terminal region together with the amphipathic EH1 helix [13,30]. While deletion of the  $\beta$ -sandwich of the P1 domain does not abolish the function of EcYidC [18], deletion of the C-terminal region (311–327) composed of two short  $\alpha$ -helices (helix 1 and helix 2) impairs cell viability and membrane insertion of a number of Sec-dependent substrates [30,31]. These two short  $\alpha$ -helices form a highly conserved interface structure (CIS), which packs against the  $\beta$ -sandwich [30]. The number and the arrangement of  $\beta$ -sheets in the P1 domain of the EcYidC are different from that of TmYidC. Accordingly, we did not use the P1 domain of EcYidC as a template for solving the structure of TmYidC by molecular replacement [30,32]. The P1 domain of TmYidC (23–224) consists of fifteen  $\beta$ -sheets, one 3/10 helix and one CIS, while the EcYidC P1 domain is composed of nineteen  $\beta$ -sheets, two 3/10 helices and one CIS. As the CIS domain and the EH1 helix contribute to the orientation of the P1 domain to the membrane [30], we used CIS as hallmark for the P1 domain orientation/conformation of the YidC protein. The position of CIS in the EcYidC insertase (PDB ID: 6AL2), is different from the EcYidC chaperone within the HTL (PDB ID: 5MG3) (Fig. 4a). The CIS of the YidC insertase is closer to the periplasmic membrane plane compared to that of the YidC chaperone within the HTL. Interestingly, helix 2 of CIS is invisible in the EcYidC chaperone within the HTL. Although the position of CIS of TmYidC is similar to that of the EcYidC insertase (Fig. 4b), helix 1 (199–205) and helix 2 (210–217) of the TmYidC do not overlay with helix 1 and helix 2 of the EcYidC (Fig. 4c). Moreover, helix 2 of TmYidC is parallel to the EH1 helix, and helix 1 forms approximately a 40-degree angle with respect to helix 2. Such an arrangement pushes the EH1 helix closer to the SecY protein (Fig. 4b and c), indicating the coupling of the P1 domain to the TM domain through the EH1 helix, which consequently modulates the interaction of YidC with SecY.

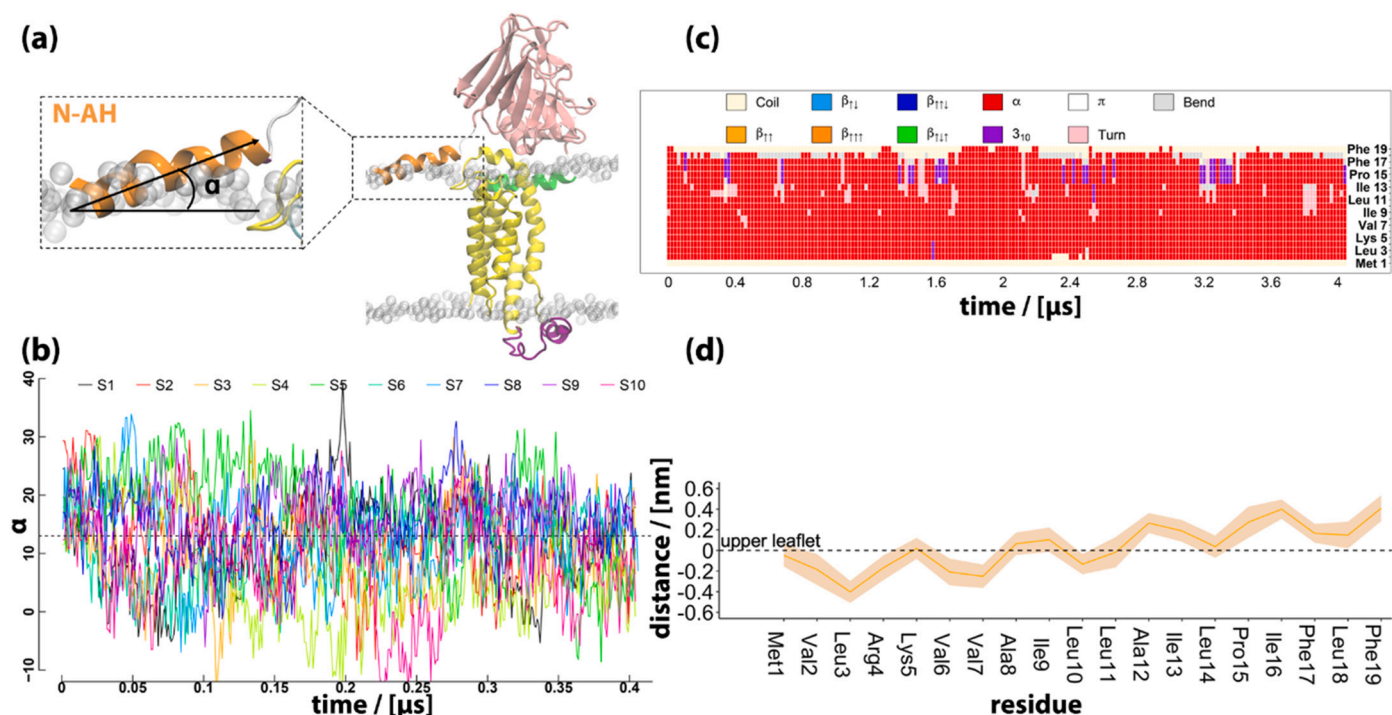


**Fig. 3.** Molecular dynamics characterization of N-AH (residues 1–19). (a) Definition of the tilt angle between N-AH and the membrane surface. The angle  $\alpha$  was calculated between a vector connecting the centers of mass of the backbone atoms of residues 2–5 and 14–17 (N-terminal turn and C-terminal turn of N-AH, respectively) and the membrane plane. (b) Time series of the angle  $\alpha$ . The horizontal dashed line represents the average over the 10 simulations. (c) Time series of the sequence profile of the secondary structure. The figure shows the cumulative sampling of 4  $\mu$ s. (d) The embedding of N-AH in the membrane is illustrated by the sequence profile of the distance between the  $C_\alpha$  atoms of N-AH and the average position of the phosphorus atoms of the phospholipids in the upper leaflet (black dashed line). The orange area represents the standard error of the mean calculated as the standard deviation of the 10 average values over the 10 individual runs.

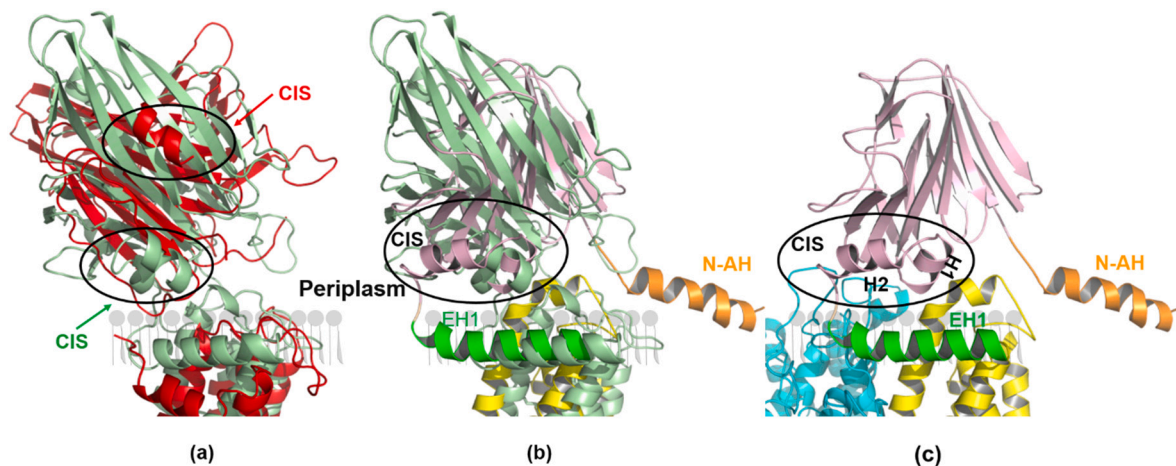


**Fig. 4.** Conformations of the P1 domain. (a) Comparison of the P1 domains of the EcYidC insertase (PDB ID: 6AL2, pale green) and the EcYidC chaperone (PDB ID: 5MG3, chain C, red). The CIS region of both structures is marked by black ellipses arrowed in pale green and red respectively. (b) Comparison of the P1 domain of the TmYidC (PDB ID: 6Y86, pink) and the EcYidC insertase (PDB ID: 6AL2, pale green). The CISs of both proteins are marked by black ellipses. (c) Position of CIS with helix 1 (H1) and helix 2 (H2) of our structure and SecY (PDB ID: 5MG3, chain Y, cyan). The structural overlap was done on the common YidC domains. (For interpretation of the references to color in this figure legend, the reader is referred to the web version of this article.)

The position and the length of the EH1 helix are important for its function as a mechanical lever to coordinate the movement of the YidC protein for releasing the nascent chain from the hydrophilic groove into the lipid bilayer [33]. The molecular dynamics simulations show that the EH1 helix of TmYidC is embedded in the lipid bilayer and aligned in a parallel fashion to the membrane surface (Fig. 5). A similar parallel arrangement, yet on the surface of the membrane, is recorded by the 11 amino acid long EH1 helix (340–351) of the EcYidC insertase (PDB ID: 6AL2). On the other hand, the EH1 helix of the EcYidC chaperone within the HTL (PDB ID: 5MG3) is inserted into the lipid bilayer and is 8 amino acids long (339–347) (Fig. 6a). The arrangement of the 18 residues of the EH1 helix of TmYidC (residues 226–244) overlaps well to those of the EcYidC insertase (Fig. 6b) and the BhYidC insertase (29–56) (Fig. 6c) indicating an insertase conformation of the EH1 helix.

#### 2.4. The C1 region of TmYidC adopts an insertase conformation

The C1 region of TmYidC (residues 282–308) has a higher B-factor in comparison to other regions of the protein, indicating that the flexibility of the C1 region is a general characteristic of the YidC protein. This result is supported by molecular dynamics simulations, which show that the C1 region records deviations up to 2.5 nm from the crystal structure (Fig. 7a). Of the two helices solved in the crystal structure (Fig. 1), only one (residues 299–308) preserves its helical conformation, whereas the second samples mainly coil and turn rich conformations (Fig. 7b). The flexibility of the C1 region in the lipid bilayer environment is shared by the BhYidC insertase, as shown in previous simulations [13].

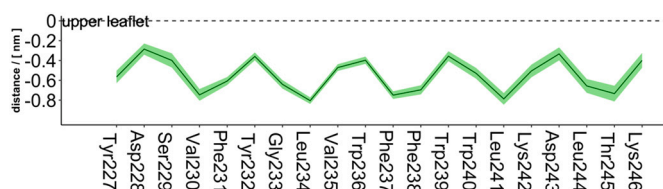


**Fig. 5.** Embedding of the EH1 helix in the membrane. The embedding is illustrated by the sequence profile of the distance between the C $\alpha$  atoms of EH1 and the average position of the phosphorus atoms of the phospholipids in the upper leaflet (black line). The green area represents the standard error of the mean calculated as the standard deviation of the 10 average values over the 10 individual runs. (For interpretation of the references to color in this figure legend, the reader is referred to the web version of this article.)

Furthermore, the structural overlap of the crystal structures of the EcYidC insertase and the EcYidC chaperone within the HTL displays evident differences in the arrangements of the CH1 and CH2 helices of the C1 region (Fig. 8a). Additionally, further comparisons of the C1 region reveal structural similarities to EcYidC and TmYidC (Fig. 8b) and structural differences to the EcYidC chaperone in the presence of SecY (Fig. 8c). For the chaperone, the C1 region of EcYidC within the HTL is in contact with SecY, while the C1 region in the insertase conformation would not interact with the SecY protein [13,28]. The diverse arrangements of the C1 region in the crystal structures and the flexibility of this domain as highlighted by the molecular dynamics simulations (Movie S1) underline its ability to switch between insertase and chaperone conformations.

#### 2.5. The hydrophilic groove of TmYidC represents an active insertase conformation

The hydrophilic groove of TmYidC encompasses TM2–TM6 and embedded in the membrane (Fig. 1a). The structure of the hydrophilic groove is conserved within the YidC/Oxa1/Alb3 family members. Comparison with all known YidC insertase structures reveals that each TM helix of the hydrophilic groove of TmYidC superimposes to the TM helices of the BhYidC (PDB ID: 3WO6) with a RMSD of 3.3 Å (Fig. 9a), and to the EcYidC (PDB ID: 6AL2) with a RMSD of 9.7 Å (Fig. 9b). The BhYidC (PDB ID: 3WO6) has been identified as an active insertase [13], suggesting that the TmYidC insertase is likely in an active conformation. This is in good agreement with reconstituted TmYidC mediating the membrane insertion of the *in vitro* synthesized c-subunit of *E. coli* ATPase (see Supplementary information Fig. S4).

#### 2.6. A structural model explaining the dual function of the YidC protein

The structural analysis of TmYidC demonstrates that the YidC protein has two fundamental structural modules. The first/basic module is a catalytic unit, i.e., the conserved hydrophilic groove required for its insertion activity. The second is the interacting module, comprising N-AH, the P1 domain, the EH1 helix and the C1 region required for the interaction with the Sec protein. The interacting module can adapt between insertase and chaperone conformations. Here, we propose a structural model to explain the insertase and chaperone conformations.

In the insertase conformation, N-AH is tilted above the periplasmic membrane, the EH1 helix is embedded in the lipid bilayer at the

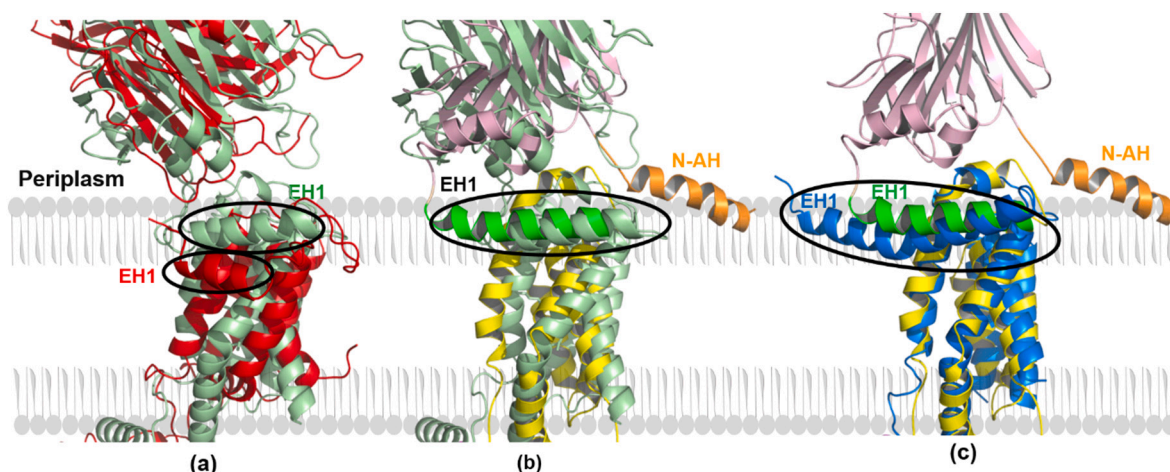


**Fig. 6.** Conformations of the EH1 helix. (a) Comparison of the EH1 helix of the EcYidC insertase (PDB ID: 6AL2, pale green) and the EcYidC chaperone (PDB ID: 5MG3, chain C, red). The EH1 helix of both structures is marked with black ellipses marked in pale green and red respectively. (b) Comparison of the EH1 helix of the TmYidC (PDB ID: 6Y86, green) and EcYidC insertase (PDB ID: 6AL2, pale green) marked in black ellipse. (c) Comparison of the EH1 helix of the TmYidC (green) and the BhYidC insertase (blue) (PDB ID: 3WO6) marked by black ellipses. (For interpretation of the references to color in this figure legend, the reader is referred to the web version of this article.)

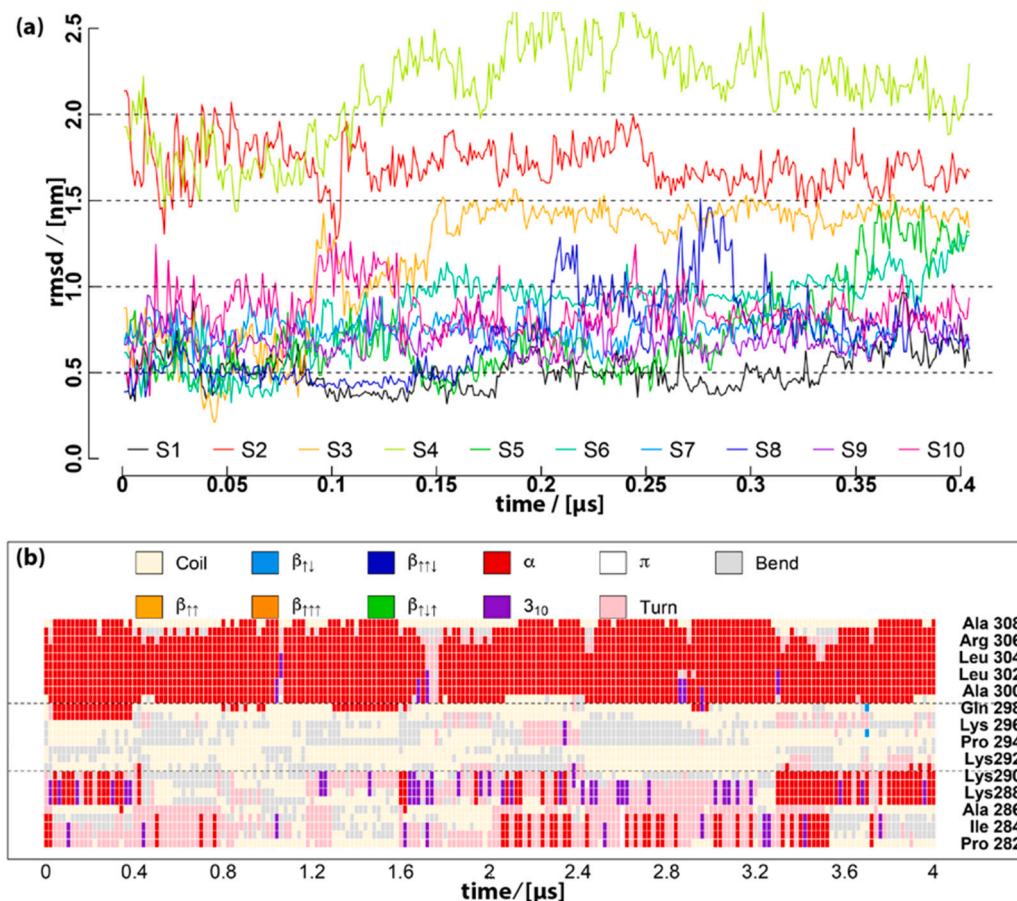


**Fig. 7.** Characterization of the C1 domain (residues 282–308). (a) Root mean square deviation of the  $C_{\alpha}$ -atoms in the C1 domain from the crystal structure (PDB ID: 6Y86). The alignment was done on the  $C_{\alpha}$ -atoms of the TM2-TM6 domain excluding the C1 region. (b) Secondary structure assignment of the residues in C1. The horizontal dashed lines separate the two helices in the crystal structure and the connecting loop.

periplasmic side arranged in a parallel fashion to the membrane surface, and the C1 region can be in the proximity of the TM3 helix of the SecY protein [10] (Fig. 10a). In the chaperone conformation, we propose that N-AH is inserted between the elements of the TMD, being able to contact

the TM7 helix of SecY. The EH1 helix is inserted into the membrane, tilted and pushed closer to SecY. The flexible C1 region can contact the N-terminal TM1 helix and the TM10 helix of SecY (Fig. 10b). This model explains how the YidC protein can function both as an insertase and as a

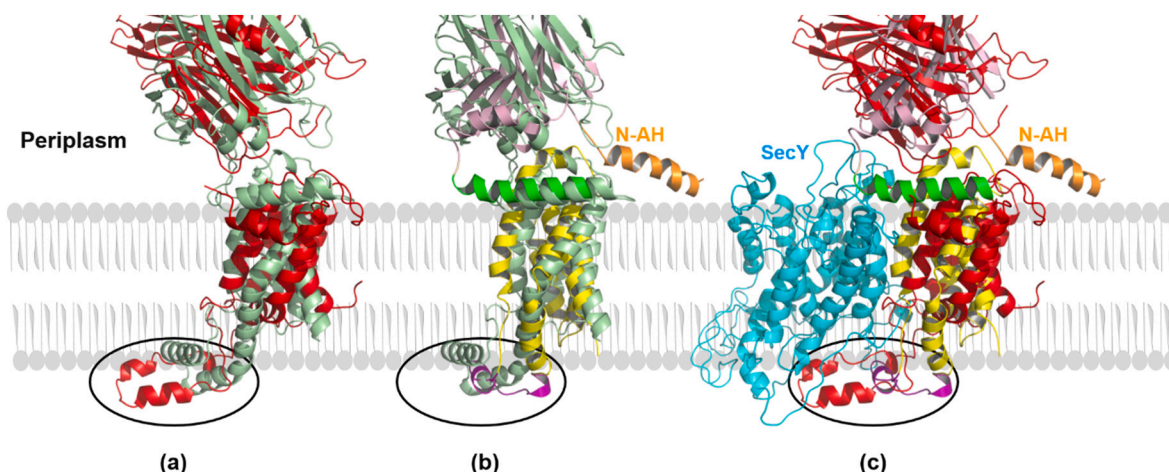


**Fig. 8.** Conformations of the C1 region (marked by the black ellipses). (a) Comparison of the C1 region of the EcYidC insertase (PDB ID: 6AL2, pale green) and the EcYidC chaperone (PDB ID: 5MG3, chain C, red). (b) Comparison of the C1 region of TmYidC (PDB ID: 6Y86, magenta) and the EcYidC insertase (PDB ID: 6AL2, pale green). (c) Comparison of the C1 region of TmYidC (magenta) and the EcYidC chaperone (PDB ID: 5MG3, chain C, red) in presence of the SecY protein (PDB ID: 5MG3, chain Y, cyan). The structural overlap was done on the common YidC domains. (For interpretation of the references to color in this figure legend, the reader is referred to the web version of this article.)

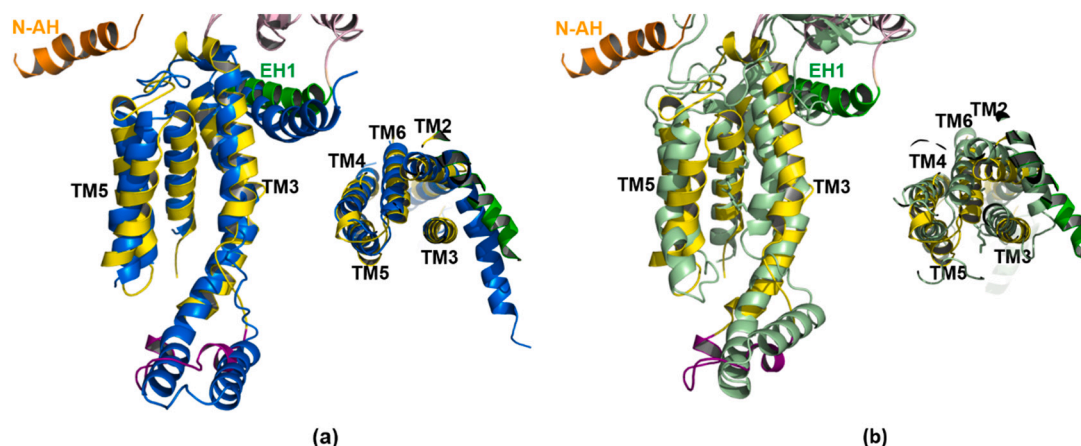


**Fig. 9.** Comparison of the TMD of TmYidC with the BhYidC insertase (PDB ID: 3WO6) and the EcYidC insertase (PDB ID: 6AL2). (a) Comparison of the TMD of TmYidC (PDB ID: 6Y86, residues 245–425, yellow) with the BhYidC insertase (PDB ID: 3WO6, blue), side and top views. For clarity, N-AH (orange) and EH1 (green) of TmYidC are also shown. (b) Comparison of the TMD of TmYidC (PDB ID: 6Y86, residues 245–425, yellow) with the EcYidC insertase (PDB ID: 6AL2, pale green), side and top views. (For interpretation of the references to color in this figure legend, the reader is referred to the web version of this article.)

chaperone by rearranging its interacting modules. N-AH can mediate the YidC insertase conformation or can promote the YidC chaperone conformation when in complex with SecY, the membrane component of the Sec translocon. For the YidC/Oxa1/Alb3 family members without N-AH, the EH1 and the C1 region could function similarly with possibly less affinity. The basic module of the YidC/Oxa1/Alb3 family of proteins can perform the insertion function with low efficiency. The interacting module of the YidC protein incorporating Sec proteins enables the insertion of diverse protein substrates and increased insertion efficiency.

### 3. Discussion and conclusions

We present a 3.4 Å-resolution structure of an active YidC insertase with the N-terminal amphipathic helix (N-AH) resolved (PDB ID: 6Y86). By maintaining the stability and functionality of the hydrophilic groove in the TM region for the insertase activity, YidC deploys its chaperone function by interacting with Sec proteins using N-AH, the P1 domain, the EH1 helix and the C1-region [10,34]. The structure solved here shows for the first time how N-AH can act as a membrane recognition helix in the insertase conformation consistent with the definition of the

AH motif [35] as well as our functional data. Furthermore, it provides the structural basis for cross-linking experiments demonstrating that N-AH is a major contacting site in the presence of SecY [10] underlining the importance of N-AH in protein-protein interactions. The presence of both N-AH and C1 in TmYidC suggests that these structural elements of the YidC protein from *T. maritima* are less flexible than those of the other YidC insertases in presence of the detergent dodecyl-maltoside (DDM). The previously published TmYidC structure did not reveal N-AH and the C1 region, which might be due to using decyl-maltoside (DM) detergent. DM might be disturbing these regions because it has a shorter alkyl chain than DDM and is therefore considered harsher [36]. The amphipathic EH1 helix connecting the P1 and TMD facilitates the coordinated movements of these domains to trigger the release of nascent chains into the membrane [33].

TmYidC is crystallized in the  $P4_1 2_1 2$  space group. In this lattice, N-AH is stabilized by crystal contacts with two symmetry related molecules in the crystal lattice. The highly hydrophobic N-AH can lie in the plane of the bilayer or insert into the lipid bilayer. During YidC biogenesis, N-AH has to be inserted into the lipid bilayer at certain points during synthesis. Whether transmembrane or surface bound, N-

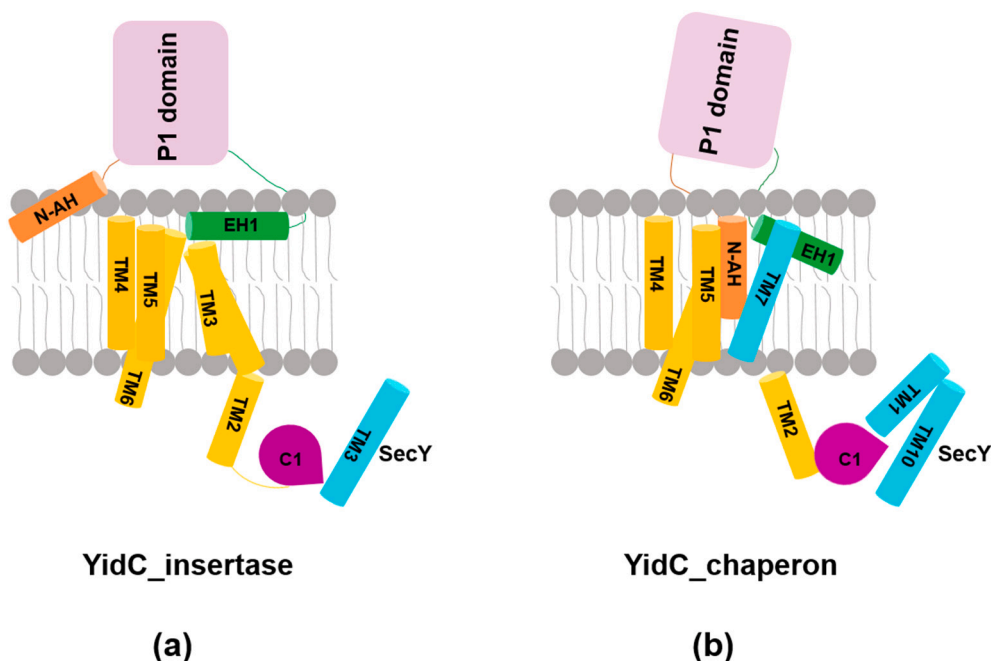


**Fig. 10.** Structural models of the YidC insertase (a) and the YidC chaperone (b) functions of Gram-negative bacteria. For clarity, only selected helices of the SecY protein are shown (cyan). (For interpretation of the references to color in this figure legend, the reader is referred to the web version of this article.)

AH could induce changes in the orientation of the P1 domain and possibly the transmembrane domain. Our MD simulations of TmYidC embedded in a POPE: POPG bilayer show that N-AH forms an angle of about 15° with the membrane surface consistent with the crystallographic observation. Furthermore, the N-terminus of N-AH is embedded in the membrane. The consequences of the tilted N-AH of TmYidC are twofold. First, the tilting may induce an insertase-compatible P1 domain and EH1 helix conformation. Second, it could make the interaction with SecY more easily. N-AH is therefore a definitory structural element, which can enable the dual-function of the YidC protein.

Combined with structural analysis of available YidC structures and molecular dynamics simulations, we propose a model that rationalizes how YidC can perform its dual function as an insertase or as a chaperone. To validate this model, the structure determination of a high-resolution YidC-SecYEG complex will be required.

## 4. Materials and methods

### 4.1. Structure determination and refinement

The structure of TmYidC was determined at 3.4 Å by molecular replacement with the crystal structure of the P1 domain of TmYidC (unpublished) using PHASER [37]. In resulting maps, additional electron density was observed, presumably for the TM domain of TmYidC. However, the electron density map was not sufficiently interpretable to build the TM domain. To improve initial phases, molecular replacement was performed using the P1 domain and TM domains of TmYidC determined separately (unpublished) as search models with the C1 region omitted. The model with the P1 domain and the TM region was placed into the additional electron density observed before and it was further rebuilt manually using COOT [38] and refined in Phenix [39]. Data collection and refinement statistics are summarized in Table 1. The atomic coordinates and structure factors were deposited in the Protein Data Bank, under the accession code 6Y86.

### 4.2. Molecular dynamics simulations

#### 4.2.1. System preparation – YidC structure

The crystal structure of TmYidC (PDB ID: 6Y86) was aligned along the membrane normal using the Orientations of Proteins in Membranes (OPM) database [40] and subsequently embedded in a 75% 1-Palmitoyl-2-oleoyl-*sn*-glycero-3-phosphoethanolamine (POPE) and 25% 1-Palmitoyl-2-oleoyl-*sn*-glycero-3-(phospho-rac-(1-glycerol)) (POPG) membrane. We used these percentages of lipid species in order to mimic the real membrane environment in which YidC is found. The full system was solvated with TIP3P water molecules [41] and 150 mM NaCl. The system consists of ~175,000 atoms in a triclinic box (~11 × 11 × 14 nm). The titratable groups of the protein were protonated according to their standard protonation states at pH 7. The preparation of the structure was done using the CHARMM-GUI webserver [42].

The initial, multi-step equilibration of the system, with a gradual release of restraints acting on protein atoms, was conducted using the scripts provided by the CHARMM-GUI. Subsequently, the system was equilibrated for 30 ns, without any restraints, prior to production runs.

#### 4.2.2. Simulation details

All simulations were performed using the GROMACS 2020.3 simulation package [43] and the CHARMM36m force field [44]. Ten independent simulations with different initial velocities were carried out cumulating 4 μs. All bonds were constrained using a fourth order LINCS algorithm [45], allowing for a 2 fs timestep. The short range interactions were cut-off beyond a distance of 1.2 nm. The long range electrostatic interactions were treated with PME [46] with a 1.2 nm real space cutoff. The systems were kept at a temperature of 303.15 K and a pressure of 1 bar, using a Nosé-Hoover thermostat [47,48] and a Parrinello-Rahman barostat [49], respectively. Periodic boundary conditions were applied and snapshots were saved every 50 ps.

Supplementary data to this article can be found online at <https://doi.org/10.1016/j.bbamem.2021.183825>.

### Data availability

Crystallographic data and coordinates were deposited in Protein

Data Bank with accession number 6Y86. All remaining data are contained within this article.

### Funding information

M.S. was supported in the framework of the BACELL EuroSCOPE program (855.01.088). A.C. is supported by an SNSF Excellence Grant (310030B-189363).

### Credit authorship contribution statement

X.L. and R.A.K. conceptualization and experimentation. K.J.N. structure determination and validation. I.M.I. and A.C. molecular dynamics simulations. M.J.S. and A.J.M.D. functional characterization. X. L., I.M.I. and A.J.M.D. making all figures. X.L. writing original draft with inputs from all co-authors.

### Declaration of competing interest

The authors declare that they have no known competing financial interests or personal relationships that could have appeared to influence the work reported in this paper.

### Data availability

Data will be made available on request.

### Acknowledgments

The PXI beamline scientists from Swiss Light Source, Villigen, Switzerland. The computational resources were provided by the Swiss National Supercomputing Centre (CSCS) in Lugano.

### References

- [1] M.J. Saller, Z.C. Wu, J. de Keyser, A.J. Driessen, The YidC/Oxa1/Alb3 protein family: common principles and distinct features, *Biol. Chem.* 393 (2012) 1279–1290.
- [2] S.A. Anghel, P.T. McGilvray, R.S. Hegde, R.J. Keenan, Identification of Oxa1 homologs operating in the eukaryotic endoplasmic reticulum, *Cell Rep.* 21 (2017) 3708–3716.
- [3] A. Guna, N. Volkmar, J.C. Christianson, R.S. Hegde, The ER membrane protein complex is a transmembrane domain insertase, *Science* 359 (2018) 470–473.
- [4] M.A. McDowell, et al., Structural basis of tail-anchored membrane protein biogenesis by the GET insertase complex, *Mol. Cell* 80 (2020) 72–86 e77.
- [5] A. Kuhn, D. Kiefer, Membrane protein insertase YidC in bacteria and archaea, *Mol. Microbiol.* 103 (2017) 590–594.
- [6] R.J. Schulze, et al., Membrane protein insertion and proton-motive-force-dependent secretion through the bacterial holo-translocon SecYEG-SecDF-YajC-YidC, *Proc. Natl. Acad. Sci. U. S. A.* 111 (2014) 4844–4849.
- [7] J. Komar, M. Botte, I. Collinson, C. Schaffitzel, I. Berger, ACCEMBLing a multiprotein transmembrane complex: the functional SecYEG-SecDF-YajC-YidC holo-translocon protein secretase/insertase, *Methods Enzymol.* 556 (2015) 23–49.
- [8] M. Botte, et al., A central cavity within the holo-translocon suggests a mechanism for membrane protein insertion, *Sci. Rep.* 6 (2016) 38399.
- [9] L. Zhu, H.R. Kaback, R.E. Dalbey, YidC protein, a molecular chaperone for LacY protein folding via the SecYEG protein machinery, *J. Biol. Chem.* 288 (2013) 28180–28194.
- [10] N.A. Petriman, et al., The interaction network of the YidC insertase with the SecYEG translocon, SRP and the SRP receptor FtsY, *Sci. Rep.* 8 (2018) 578.
- [11] J. Komar, et al., Membrane protein insertion and assembly by the bacterial holo-translocon SecYEG-SecDF-YajC-YidC, *Biochem. J.* 473 (2016) 3341–3354.
- [12] A. Kuhn, H.G. Koch, R.E. Dalbey, Targeting and insertion of membrane proteins, *EcoSal Plus* 7 (2017).
- [13] K. Kumazaki, et al., Structural basis of sec-independent membrane protein insertion by YidC, *Nature* 509 (2014) 516–520.
- [14] K. Kumazaki, et al., Crystal structure of *Escherichia coli* YidC, a membrane protein chaperone and insertase, *Sci. Rep.* 4 (2014) 7299.
- [15] Y. Chen, R. Soman, S.K. Shanmugam, A. Kuhn, R.E. Dalbey, The role of the strictly conserved positively charged residue differs among the Gram-positive, gram-negative, and chloroplast YidC homologs, *J. Biol. Chem.* 289 (2014) 35656–35667.
- [16] Y. Geng, et al., Role of the cytosolic loop C2 and the C terminus of YidC in ribosome binding and insertion activity, *J. Biol. Chem.* 290 (2015) 17250–17261.
- [17] F. Jiang, et al., Chloroplast YidC homolog Albino3 can functionally complement the bacterial YidC depletion strain and promote membrane insertion of both bacterial and chloroplast thylakoid proteins, *J. Biol. Chem.* 277 (2002) 19281–19288.
- [18] F. Jiang, et al., Defining the regions of *Escherichia coli* YidC that contribute to activity, *J. Biol. Chem.* 278 (2003) 48965–48972.
- [19] I. Sachelaru, et al., YidC and SecYEG form a heterotetrameric protein translocation channel, *Sci. Rep.* 7 (2017) 101.
- [20] S.U. Heinrich, T.A. Rapoport, Cooperation of transmembrane segments during the integration of a double-spanning protein into the ER membrane, *EMBO J.* 22 (2003) 3654–3663.
- [21] E.N. Houben, C.M. ten Hagen-Jongman, J. Brunner, B. Oudega, J. Lührink, The two membrane segments of leader peptidase partition one by one into the lipid bilayer via a Sec/YidC interface, *EMBO Rep.* 5 (2004) 970–975.
- [22] T. Hessa, et al., Recognition of transmembrane helices by the endoplasmic reticulum translocon, *Nature* 433 (2005) 377–381.
- [23] H. Sadlish, D. Pitonzo, A.E. Johnson, W.R. Skach, Sequential triage of transmembrane segments by Sec61alpha during biogenesis of a native multispanning membrane protein, *Nat. Struct. Mol. Biol.* 12 (2005) 870–878.
- [24] T. Hessa, et al., Molecular code for transmembrane-helix recognition by the Sec61 translocon, *Nature* 450 (2007) 1026–1030.
- [25] K. Hatzixanthis, T. Palmer, F. Sargent, A subset of bacterial inner membrane proteins integrated by the twin-arginine translocase, *Mol. Microbiol.* 49 (2003) 1377–1390.
- [26] S. Wickles, et al., A structural model of the active ribosome-bound membrane protein insertase YidC, *elife* 3 (2014), e03035.
- [27] M.T. Borowska, P.K. Dominik, S.A. Anghel, A.A. Kossiakoff, R.J. Keenan, A YidC-like protein in the archaeal plasma membrane, *Structure* 23 (2015) 1715–1724.
- [28] Y. Tanaka, et al., 2.8-Å crystal structure of *Escherichia coli* YidC revealing all core regions, including flexible C2 loop, *Biochem. Biophys. Res. Commun.* 505 (2018) 141–145.
- [29] Y. Xin, et al., Structure of YidC from *thermotoga maritima* and its implications for YidC-mediated membrane protein insertion, *FASEB J.* 32 (2018) 2411–2421.
- [30] S. Ravaut, G. Stjepanovic, K. Wild, I. Sinning, The crystal structure of the periplasmic domain of the *Escherichia coli* membrane protein insertase YidC contains a substrate binding cleft, *J. Biol. Chem.* 283 (2008) 9350–9358.
- [31] K. Xie, D. Kiefer, G. Nagler, R.E. Dalbey, A. Kuhn, Different regions of the nonconserved large periplasmic domain of *Escherichia coli* YidC are involved in the SecF interaction and membrane insertase activity, *Biochemistry* 45 (2006) 13401–13408.
- [32] D.C. Oliver, M. Paetzel, Crystal structure of the major periplasmic domain of the bacterial membrane protein assembly facilitator YidC, *J. Biol. Chem.* 283 (2008) 5208–5216.
- [33] A. Kedrov, et al., Structural dynamics of the YidC: ribosome complex during membrane protein biogenesis, *Cell Rep.* 17 (2016) 2943–2954.
- [34] I. Sachelaru, et al., YidC occupies the lateral gate of the SecYEG translocon and is sequentially displaced by a nascent membrane protein, *J. Biol. Chem.* 288 (2013) 16295–16307.
- [35] J.P. Segrest, H. Deloof, J.G. Dohlman, C.G. Brouillette, G.M. Anantharamaiah, Amphipathic helix motif - classes and properties, *Proteins-Struct. Funct. Genet.* 8 (1990) 103–117.
- [36] G.G. Prive, Detergents for the stabilization and crystallization of membrane proteins, *Methods* 41 (2007) 388–397.
- [37] A.J. McCoy, et al., Phaser crystallographic software, *J. Appl. Crystallogr.* 40 (2007) 658–674.
- [38] P. Emsley, B. Lohkamp, W.G. Scott, K. Cowtan, Features and development of coot, *Acta Crystallogr. D Biol. Crystallogr.* 66 (2010) 486–501.
- [39] P.D. Adams, et al., PHENIX: a comprehensive Python-based system for macromolecular structure solution, *Acta Crystallogr. D Biol. Crystallogr.* 66 (2010) 213–221.
- [40] M.A. Lomize, I.D. Pogozheva, H. Joo, H.I. Mosberg, A.L. Lomize, OPM database and PPM web server: resources for positioning of proteins in membranes, *Nucleic Acids Res.* 40 (2012) D370–D376.
- [41] W.L. Jorgensen, J. Chandrasekhar, J.D. Madura, R.W. Impey, M.L. Klein, Comparison of simple potential functions for simulating liquid water, *J. Chem. Phys.* 79 (1983) 926–935.
- [42] S. Jo, T. Kim, V.G. Iyer, W. Im, CHARMM-GUI: a web-based graphical user interface for CHARMM, *J. Comput. Chem.* 29 (2008) 1859–1865.
- [43] D. Van Der Spoel, et al., GROMACS: fast, flexible, and free, *J. Comput. Chem.* 26 (2005) 1701–1718.
- [44] J. Huang, et al., CHARMM36m: an improved force field for folded and intrinsically disordered proteins, *Nat. Methods* 14 (2017) 71–73.
- [45] B. Hess, H. Bekker, H.J.C. Berendsen, J.G.E.M. Fraaije, LINCS a linear constraint solver for molecular simulations, *J. Comput. Chem.* 18 (1997).
- [46] H.J.C. Berendsen, J.P.M. Postma, W.F. van Gunsteren, A. DiNola, J.R. Haak, Molecular dynamics with coupling to an external bath, *J. Chem. Phys.* 81 (1984) 3684–3690.
- [47] S. Nosé, A unified formulation of the constant temperature molecular dynamics methods, *J. Chem. Phys.* 81 (1984) 511–519.
- [48] W.G. Hoover, Canonical dynamics: equilibrium phase-space distributions, *Phys. Rev. A Gen. Phys.* 31 (1985) 1695–1697.
- [49] M. Parrinello, A. Rahman, Polymorphic transitions in single crystals: a new molecular dynamics method, *J. Appl. Phys.* 52 (1981).